



Application of second-order geoelectric indices in determination of groundwater vulnerability in hard rock terrain in SW. Nigeria

Victor Olumuyiwa Akinseye¹ · Wasiu Olajuwon Osisanya² · Moses Oghenenyoreme Eyankware^{3,4} · Isaac Akinjide Korode⁵ · Abel Taiwo Ibitoye⁵

Received: 12 October 2022 / Accepted: 28 August 2023 / Published online: 22 September 2023
© The Author(s), under exclusive licence to Springer Nature Switzerland AG 2023

Abstract

The application of the VES geophysical technique to investigate groundwater potential and the aquifer vulnerability was carried out at Akure, southwestern part of Nigeria. Sixteen (16) VES points were selected using a Schlumberger array applied for the conduction of the VES. The ABEM Terrameter SAS 1000 was used and the maximum current electrode spacing (AB/2) was 100 m. A partial curve matching technique and computer iteration technique were applied in the interpretation of data using WINRESIST software, while Groundwater Modeling System (GMS) software was used to model the groundwater flow direction. The study revealed the presence of two to four layers of curve types, which include H (69%), HKH (19%), A (6%), and QH (6%) respectively. The second-order geoelectric parameters include longitudinal conductance (S), average transverse resistance (Tr), average longitudinal resistance (ρ_L), coefficient of anisotropy (λ), reflection coefficient (R_c), and resistivity contrast (F_c). The estimated aforementioned parameters range 0.004–1.03, 659.6–12,416.6 Ω/m^2 , 28.21–267.4 $\Omega\cdot m$, 58.82–303.26, 1–1.5, 0.33–0.97, and 2.01–57.33, respectively. The distributions of these parameters are revealed by the contour maps, which aid in the delineation of zones with different layer characteristics. The findings of this study can be used as a guide for making decisions on groundwater abstraction and management.

Keywords Basement · Aquifer · Resistivity · Protective capacity · Akure · Nigeria

Introduction

About 98% of the world's freshwater is found underground, and it is distributed rather evenly around the globe. It provides a reliable, consistent supply that is not fully prone to drying out in natural conditions, such as surface water (UNESCO 2022). However, the preferred source of drinking water globally is groundwater, which is often considerably

more dependable than surface water, and easily accessible by consumers (Carrarad et al. 2019; Eyankware and Akakuru 2022). Water resource quality is deteriorating worldwide due to several issues. Anthropogenic activities, in particular within the study area, are one of the key variables that affect water quality. Various fields of research, including geology, microbiology, biochemistry, and others, have continued to examine the gradual decline in water quality (Obasi et al. 2022). A detail knowledge of geology and hydrogeology of the study area are very necessary for reliable interpretation (Abiola et al. 2009). To learn about the subsurface lithology and aquiferous zones, such as fractures, faults, and joints, which are favorable to groundwater accumulation and groundwater quality, complete geophysical research is frequently required before groundwater exploitation. The lack of sufficient data coverage for groundwater development and management, however, frequently places restrictions on geophysical research and other conventional techniques such as geostatistical and numerical modeling (Eyankware et al. 2022). The appraisal of groundwater potential and the vulnerability of aquifers in typical basement complex terrains

✉ Wasiu Olajuwon Osisanya
wasuu.osisanya@uniben.edu

¹ Department of Applied Geophysics, Federal University of the Technology, Akure, Nigeria

² Department of Physics, University of Benin, Benin City, Edo State, Nigeria

³ Department of Geology, Dennis Osadabey University, Anwai, Asaba, Delta State, Nigeria

⁴ GeoMoses Consultancy Limited Warri, Warri, Delta State, Nigeria

⁵ Department of Petroleum Engineering and Geosciences, Petroleum Training Institute, Effurun, Nigeria

have been the subject of much research worldwide (Akindeji 2020; Akintorinwa 2015; Joel et al. 2016). For the evaluation of groundwater potential, these studies frequently used geoelectrical and hydrogeological characteristics such as aquifer resistivity, aquifer thickness, hydraulic conductance, and transmissivity separately. The application of geophysics in the analysis of aquifer vulnerability has recently become popular (Eyankware et al. 2022; Umayah and Eyankware 2022; Eyankware and Aleke 2021). Groundwater distribution, aquifer vulnerability, and building foundations, among other things, can all be determined using geophysical techniques, especially electric resistivity methods. Eyankware et al. (2022) and Eyankware and Aleke (2021) employed geophysical instruments for groundwater investigations Al-Garni et al. (2005), Eyankware and Umayah (2022). Similarly, numerous geophysical approaches can be used to search for groundwater resources, including electrical resistivity, seismic, gravity, and ground-penetrating radar (Kearey et al. 2002). The electrical resistivity approach utilizing vertical electrical sounding and Schlumberger electrode array can be used to investigate the spatial distribution and depth of various hydro-lithostratigraphic units (Ebong et al. 2016; Akpan et al. 2013, 2014). This procedure is quick, inexpensive, non-invasive, and environmentally friendly (Ebong et al. 2016), and the necessary equipment is easily accessible. However, such data are occasionally linked with mistakes resulting from inherent uncertainties in the transfer of electrical resistivity data to geology models (Ebong et al. 2014). The ambiguities are usually resolved by combining geology and geophysical data (Ebong et al. 2016). Aside from the aforementioned drawbacks, the electrical resistivity approach cannot be used to investigate depths more than 1000 m (Kearey et al. 2002), though earlier research in the research area revealed that the depth of water-carrying units was less than 1000 m (Abiola et al. 2009; Olorunfemi and Fasuyi 1993). Studies have not been carried out within the study area to the best of our knowledge on aquifer vulnerability and groundwater flow direction. Groundwater models are crucial for the development and management of groundwater resources as well as for foretelling the outcomes of management actions. Groundwater modeling has evolved into a common instrument for expert hydrogeologists to efficiently carry out the majority of jobs because of the significant gains in computation power and the widespread availability of computers and model software. Models of groundwater flow have been used to investigate the dynamics of groundwater systems and comprehend flow patterns. However, all the previous published research used the one-time dataset to map the output. However, these do not depict the true representation of the groundwater flow direction. This research will serve as a baseline; similarly, this paper has highlighted groundwater flow direction using GMS and devised appropriate management of the Akure

aquifer. Although the present paper has focused on a small area of Akure, the results apply to a wide range. Akure aquifer is very large and has almost similar aquifer parameters throughout. Furthermore, the focus of this research is on assessing aquifer vulnerability and also inferring aquifer potential within the study area.

Location, accessibility, and physiographic of the study area

The study area is located between latitudes $7^{\circ} 11' N$ and $7^{\circ} 18' N$, and longitudes $5^{\circ} 9' E$ and $5^{\circ} 19' E$ see Fig. 1. The study area covers a total area of about 2.5 km^2 . The area is accessible via Oba-Ile estate from NTA road. The entire research area is connected to the NTA road by an unpaved motorable road. The location is bordered by granitic rock outcroppings and is situated on gently undulating terrain. The elevation varies between 303 and 335 m. It rains throughout the year at Oba-Ile Akure, but the commencement is in March and the cessation (severe decrease in amount) is in November, according to the available rainfall data. The yearly rainfall ranges from 1150 mm in the north to 2000 mm in the south. As you move inland from the shore, the amount and distribution of rainfall decrease (Akinseye 2010; Akinseye et al. 2012). It was reported by Ayolabi et al. (2003) that the study area is characterized by bedrock depression and bedrock ridges with structural fault zones viable for suitable groundwater establishment. Adedipe et al. (2014) also conducted a geophysical investigation in the study area with the intent of assessing its groundwater potential as well as appraising its aquifer protection capacity. It was recommended that low- to medium-capacity borehole can be established in the study area and that the aquifer is safe. Eebo and Yusuf (2021) discovered from their research on the study area that it is characterized by a medium aquifer and very few parts are non-aquiferous.

Geology of the study area

The study area is underlain by the Precambrian Basement complex rocks of Southwestern Nigeria (Rahaman 1988), which are divided into two primary petrologic units: biotite–granite and migmatite gneiss; see Fig. 1. In the western part of this research area, outcrops of biotite gneiss and granitic gneiss can be found. Similarly, charnokites and granite boulders may be found along the study area's western street. Weathering processes form surface layers with various degrees of porosity and permeability, which are found in typical basement topography (Odunsanya and Amadi 1990) in tropical and equatorial locations.

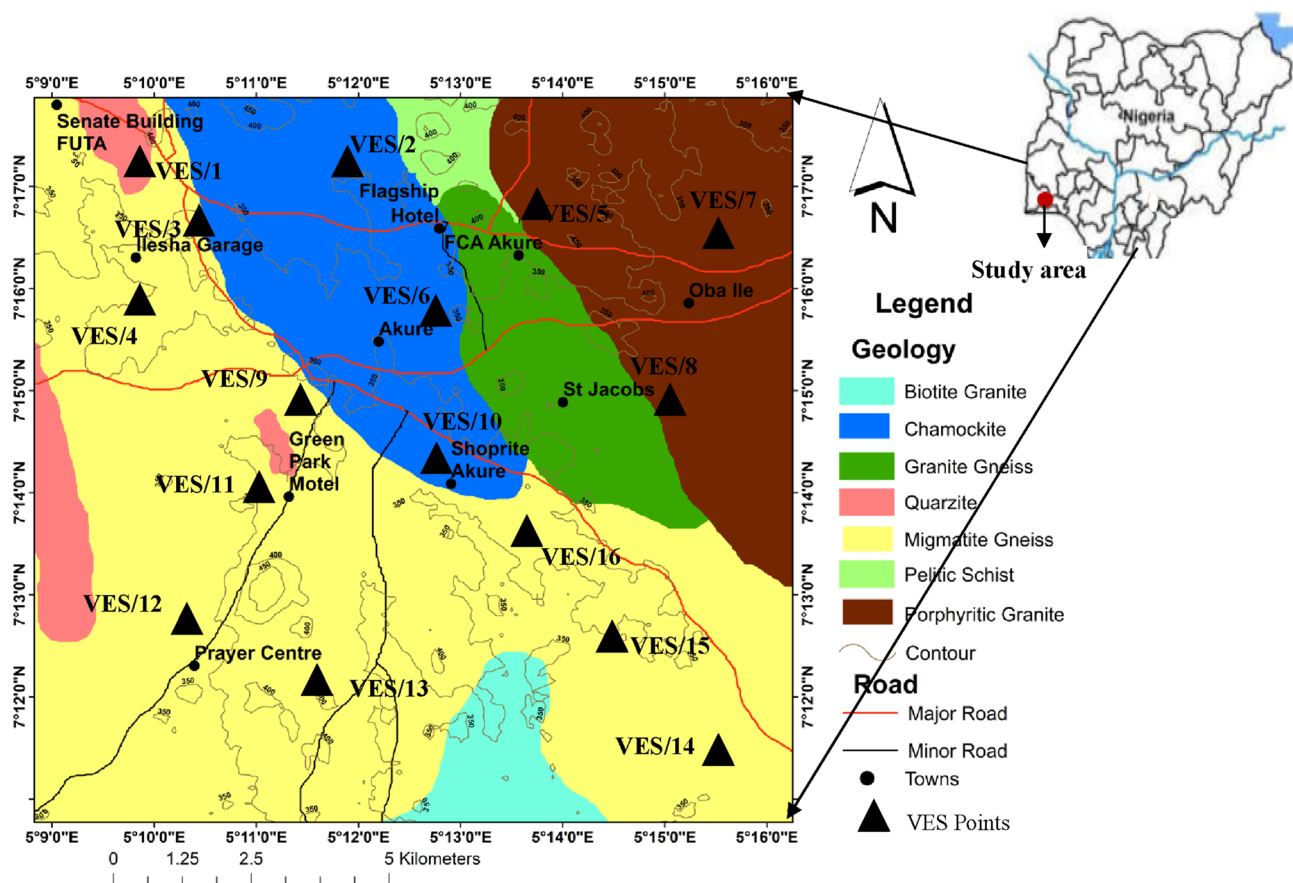


Fig. 1 Geology map of the study area showing VES points

Hydrogeology of the study area

Groundwater in Nigeria is restricted by the fact that more than half of the country is underlain by crystalline basement rock of the Precambrian era (Kazeem 2007). The main rock types in this geological terrain include igneous and metamorphic rocks such as migmatites and granite gneisses. Dan-Hassan and Olorunfemi (1999) used the electrical resistivity method to delineate different subsurface geoelectrical layers, aquifer unit and their characteristics, the subsurface structure, and its influence on the general hydrogeological condition in the north-central part of Kaduna state, Nigeria. According to previous authors, locating water-bearing units in an area underlain by basement complicated rocks is a difficult undertaking in general (Aboh and Osazuwa 2000; Olorunfemi and Fasuyi 1993). Exploration for groundwater is difficult due to the great variety in lithology and structure, as well as extremely localized water-producing zones (Abiola et al. 2009; Olorunfemi et al. 1999; Oladapo et al. 2004). High topographical features that are associated with high bedrock relief are among the elements that are examined for a well site in basement complex locations (e.g., ridges). In some places, this is a crucial consideration for well location.

Because bedrock ridges' crests (when present) act as a radiating center for groundwater as water normally drains along steep slopes and hilltops to a point of discharge in adjacent lowlands, wells located on flat terrain and valleys tend to yield more water than wells located on hilltops and valley sides (Olorunfemi and Okhue 1992). Fault breccias can be used to locate well locations in metamorphic terrains (Olorunfemi and Okhue 1992). When features like as a reef cut across a small piece of a valley with a high recharge area, hornblende gneiss and connected with basic dykes act as barriers to groundwater flow, and perfect conditions exist (Akakuru et al. 2023).

However, both intergranular and fracture porosities can be seen in weathered rocks. The weathered portion's clay composition reduces permeability to some amount. Weathered and fracture aquifers in hard rock areas are capable of providing enough water to support the demands of a small hamlet or village (Patrick et al. 2021). Weathered, partially weathered/fractured zones in crystalline rocks generate aquifers (Olorunfemi and Okhue 1992). Weathering varies in nature and degree and is primarily determined by the presence of fractures at depth and favorable morphological features at the surface.

Methodology

Geoelectrical measurements

Sixteen (16) VES were conducted within the study area, as shown in Fig. 1, with the help of an OHMEGA Terrameter and its accessories. For each VES profile, a Schlumberger electrode array was used with a maximum half current (AB/2) electrode separation of 100 m and a half potential (MN/2) electrode separation of 5 m. Surfer software was used to map the spatial distribution of S , Tr , ρ_L , and ρ_t . The following Eq. (1) was used to convert the observed field data to apparent resistivity (a) values:

$$\frac{\pi \left(\left(\frac{AB}{2} \right) - \left(\frac{MN}{2} \right) \right) \Delta V}{I} \tag{1}$$

The geoelectrical curves were generated by plotting the apparent resistivity data against the current electrode spacing (AB/2). The data processing was aided by the use of WINRESIST software, which allowed for the creation of sound curves. The groundwater flow direction was generated with the use of groundwater modeling system software (GMS) which utilizes the geographic coordinates and elevation (topographic nature) of the study area aside from other relevant data such as hydraulic conductivity of the geology formation present, well, river, recharge, lake, and stream information if available. The thickness of the aquifer was calculated using the geoelectrical sections, which were produced using the information from the sounding curves. The charts supplied by Loke (1999) and Kearey et al. (2002) were used to deduce lithologies that corresponded to the geoelectric section. For the analysis and comprehension of the geologic model, some factors linked to the different combinations of thickness and resistivity of the geoelectric layer are crucial (Zohdy et al. 1974; Mailliet 1947). Dar Zarrouk's longitudinal (S) and transverse (T) parameters were derived via:

$$S = \frac{h}{p}, \tag{2}$$

$$T = hp, \tag{3}$$

where h is the aquifer thickness and p is the aquifer resistivity.

Longitudinal unit conductance (S) was calculated using Eq. (4).

The longitudinal conductance is equal to the number of layers (n).

$$S = \sum_{i=1}^n \frac{h_i}{\rho_i} = \frac{h_1}{\rho_1} + \frac{h_2}{\rho_2} + \dots + \frac{h_n}{\rho_n}, \tag{4}$$

as proposed by Asfahani (2013) and Durotoye et al. (2022).

Transverse unit resistance (Tr) was calculated using Eq. (5).

The total resistance of the transverse unit is:

$$Tr = \sum_{i=1}^n h_i \rho_i = h_1 \rho_1 + h_2 \rho_2 + \dots + h_n \rho_n, \tag{5}$$

as proposed by Oli et al. (2021), Nwachukwu et al. (2019).

Longitudinal resistance was calculated using Eq. (6).

$$\rho_L = \frac{H}{S} = \frac{\sum_{i=1}^n h_i}{\sum_{i=1}^n \frac{h_i}{\rho_i}}, \tag{6}$$

as proposed by Suneetha and Gupta (2018).

Transverse resistance was determined from Eq. (7).

$$\rho_t = \frac{T}{H} = \frac{\sum_{i=1}^n h_i \rho_i}{\sum_{i=1}^n h_i}, \tag{7}$$

as proposed by Suneetha and Gupta (2018).

The coefficient of anisotropy is a useful parameter of an anisotropic medium which indicates the degree of fracturing. It was determined using Eq. (8):

$$\lambda = \sqrt{\frac{\rho_t}{\rho_L}} = \frac{\sqrt{ST}}{H}. \tag{8}$$

The reflection coefficient (R_c) and resistivity contrast (F_c) were calculated using Eqs. (9) and (10), respectively.

As proposed by Umayah and Eyankware (2022) and Olanunjoye and Jekayinfa (2015):

$$R_c = \frac{\rho_n - \rho_{n-1}}{\rho_n + \rho_{n-1}}, \tag{9}$$

$$F_c = \frac{\rho_n}{\rho_{n-1}}, \tag{10}$$

where ρ_n is the layer resistivity of the n th layer, and ρ_{n-1} is the layer resistivity overlying the n th layer.

Results and discussion

Table 1 shows the results of the interpreted VES survey.

Dar Zarrouk parameter of the study area

Longitudinal unit conductance (S), transverse unit resistance (Tr), average longitudinal resistance (ρ_L), transverse resistivity (ρ_t), coefficient of anisotropy (λ), reflection coefficient

Table 1 The processed VES data utilized to create curve-type geoelectric layers

VES latitude longitude	Resistivity (Ωm)					Layer depth (m)					Curve type	No. of layers		
	ρ_1	ρ_2	ρ_3	ρ_4	ρ_5	d_1	d_2	d_3	d_4	d_5				
VES 01	7° 17' 43" N	5° 9' 50"E	324.3	124.9	207.5	96.8	721.2	0.8	3.8	15.8	24.2	∞	HKH	5
VES 02	7° 17' 43" N	5° 11' 56"E	321.7	93.7	282.0	73.9	827.8	0.9	3.4	12.2	35.6	∞	HKH	5
VES 03	7° 16' 50" N	5° 10' 20"E	265.4	37.3	245.4	∞	∞	2.1	10.7	∞			H	3
VES 04	7° 16' 05" N	5° 9' 56"E	779.1	127.1	1532	∞	∞	4.5	27.9	∞			H	3
VES 05	7° 17' 00"N	5° 13' 45"E	701.2	99.7	325.2	∞	∞	2.5	19.1	∞			H	3
VES 06	7° 16' 00"N	5° 12' 50"E	427.6	47.3	203.6	∞	∞	2.5	10.4	∞			H	3
VES 07	7° 16' 55"N	5° 15' 40"E	296.6	26.1	1443.9	∞	∞	1.5	10.9	∞			H	3
VES 08	7° 15' 10"N	5° 15' 05"E	283.3	24.7	277.3	∞	∞	1.5	9.5	∞			H	3
VES 09	7° 15' 05"N	5° 11' 20"E	62.6	86.2	1077.1	∞	∞	1.9	23.8	∞			A	3
VES 10	7° 14' 30"N	5° 12' 45"E	251.3	43.0	359.3	61.2	562.2	2.6	7.5	23.7	47.8		HKH	5
VES 11	7° 14' 20"N	5° 11' 00"E	232.1	38.3	2195.9	∞	∞	2.8	12.5	∞			H	3
VES 12	7° 12' 58"N	5° 10' 15"E	605.0	239.0	479.3	∞	∞	2.3	10.8	∞			H	3
VES 13	7° 12' 30"N	5° 11' 25"E	614.2	84.4	40.1	121.6	∞	1.4	7.0	18.8			QH	4
VES 14	7° 11' 40"N	5° 15' 20"E	297.2	42.4	859.3	∞	∞	1.7	14.1	∞			H	3
VES 15	7° 13' 50"N	5° 14' 10"E	249.3	32.6	625.6	∞	∞	2.0	9.3	∞			H	3
VES 16	7° 13' 40"N	5° 13' 40"E	422.9	59.7	233.0	∞	∞	23.3	15.2	∞			H	3

Table 2 Results of second-order geoelectric indices

VES points	Longitudinal unit conductance (S), mhos	Transverse unit resistance (Tr), Ω/m^2	Average longitudinal resistance (ρ_L) $\Omega\text{-m}$	Transverse resistivity (ρ_t)	Coefficient of anisotropy (λ)	Reflection coefficient (R_c)	Resistivity contrast (F_c)
VES/1	0.359036	6355.12	124.22	142.49	1.07	0.76	7.45
VES/2	0.564078	6679.35	92.36	128.2	1.18	0.84	11.2
VES/3	0.294776	956.45	43.42	74.72	1.31	0.74	6.58
VES/4	0.225288	7052.04	143.82	217.66	1.23	0.85	12.05
VES/5	0.19514	3657.27	110.69	169.32	1.24	0.53	3.26
VES/6	0.22572	1560.92	57.15	121	1.46	0.62	4.3
VES/7	0.422682	729.39	29.34	58.82	1.42	0.96	55.32
VES/8	0.38991	659.6	28.21	59.96	1.46	0.84	11.23
VES/9	0.306454	2170.5	83.86	84.46	1	0.85	12.5
VES/10	1.031772	12,416.65	79.09	152.16	1.39	0.8	9.19
VES/11	0.338435	1128.63	45.21	73.77	1.28	0.97	57.33
VES/12	0.04899	3972.7	267.4	303.26	1.06	0.33	2.01
VES/13	0.554046	2204.56	49.09	81.05	1.28	0.94	30.33
VES/14	0.338267	1103.08	46.71	69.82	1.22	0.91	20.27
VES 15	0.2932	801.78	38.53	70.95	1.35	0.9	19.19
VES16	0.309	10,761.01	124.31	279.51	1.5	0.59	3.9
Min	0.04899	659.6	28.21	58.82	1	0.33	2.01
Max	1.031772	12,416.65	267.4	303.26	1.5	0.97	57.33
Aver	0.387642	4182.517	92.16778	136.0683	1.275	0.762778	18.08056

(R_c), and resistivity contrast (F_c) were calculated. The results are obtained from primary resistivity parameters such as resistivity thickness and depth using Eqs. (4–10). The calculated results are presented in Table 2.

Longitudinal unit conductance (S)

Longitudinal conductance can help to define the degree of groundwater protection from vertical infiltration of pollutants (Oni et al. 2017). It is the conductance in the direction

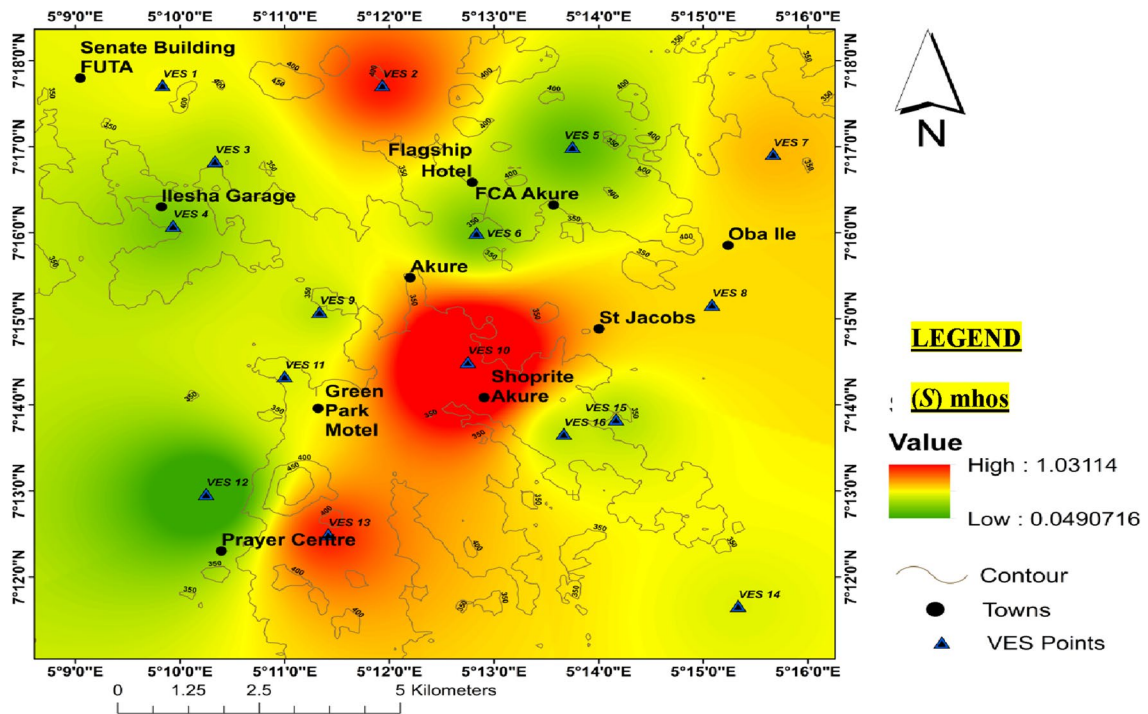


Fig. 2 Spatial variation of longitudinal conductance across the study area

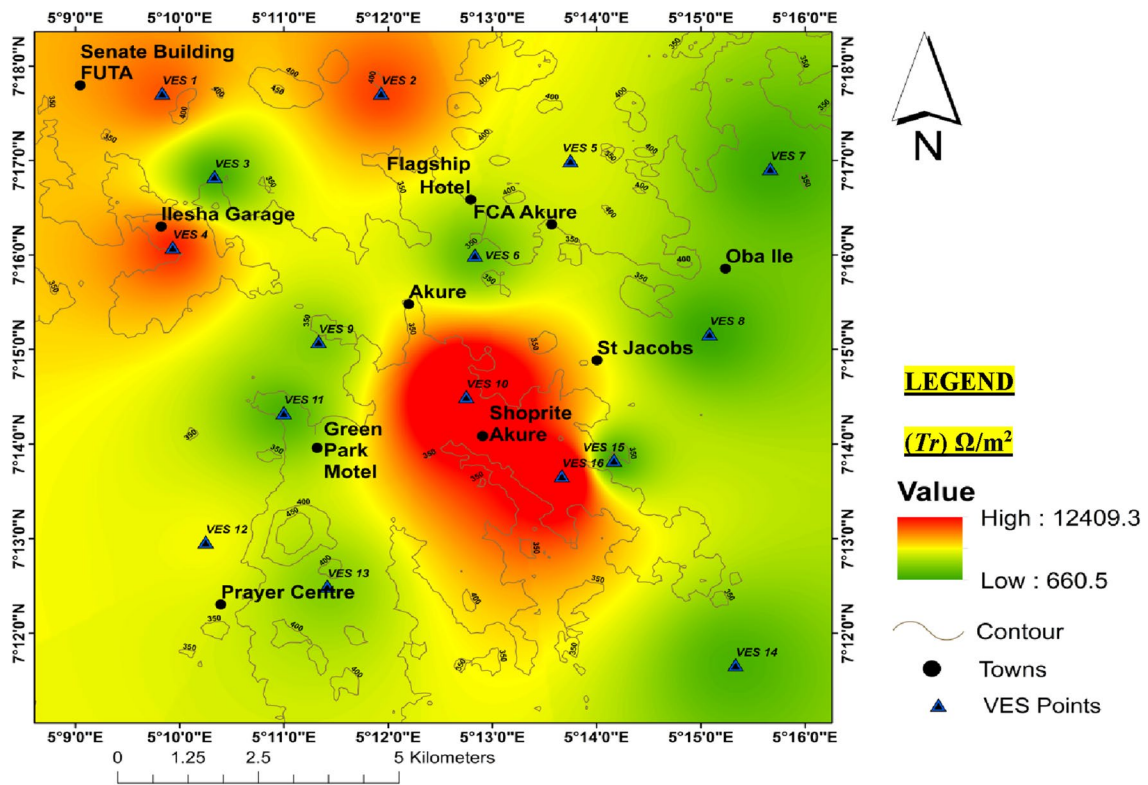


Fig. 3 Spatial distribution map of transverse unit resistance

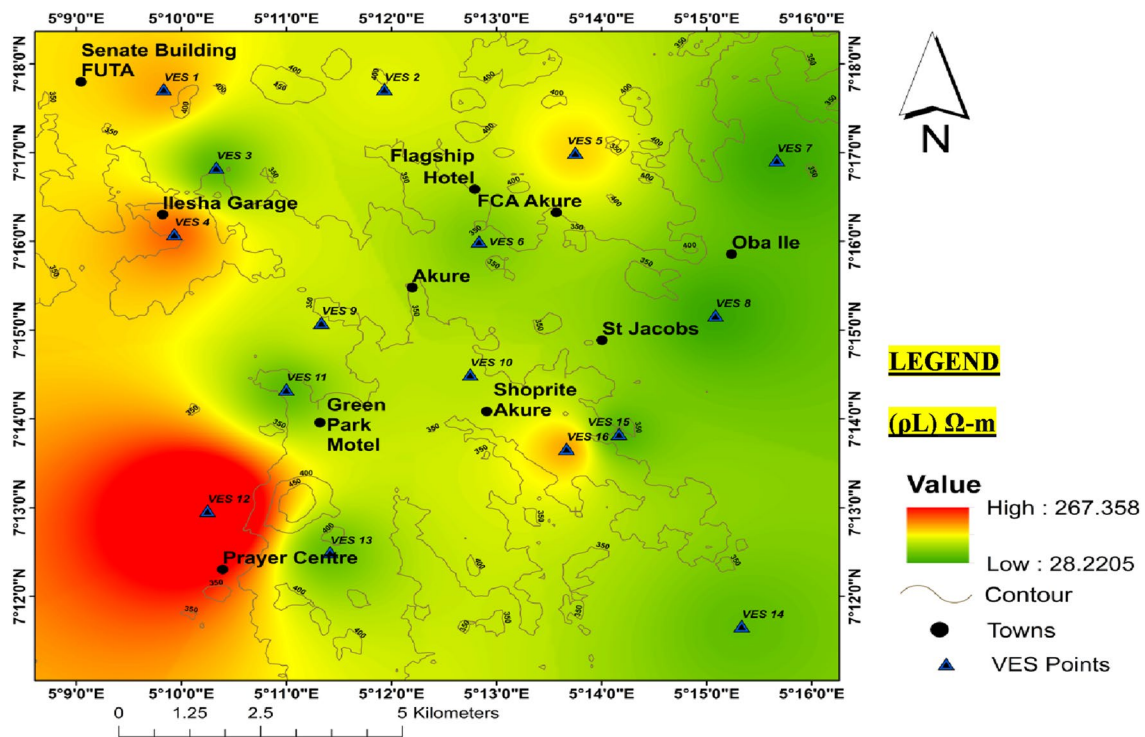


Fig. 4 Spatial distribution map of average longitudinal resistance

of the bedding plane through a column of 1 m. It is denoted by S (Nwanko et al. 2011). Oladapo and Akintorinwa (2007) and Henriet (1976) stated that geologic formations with longitudinal conductance greater than $10 \Omega^{-1}$ can be rated to have excellent aquifer protective capacity, while formations with $(5-10) \Omega^{-1}$ are rated very good, formations with $(0.7-4.9) \Omega^{-1}$ are rated good, formations with $(0.2-0.69)$ mhos are moderate, formations with $(0.1-0.19)$ mhos weak and formations with less than $0.1 \Omega^{-1}$ are poor. Hence, it could be inferred that VES 1, 2, 3, 4, 6, 7, 8, 9, 10, 11, 13, 14, 15, and 16, VES 5, and VES 12 fell within the moderate, weak, and poor, respectively, based on aquifer protective rating capacity. This also connotes that 88% of the sounding points (VES points) are expected to be of moderate aquiferous protective capacity and 6% could be weak, while the remaining 6% is rated poor. This is contrary to the observation of Akinrinade and Adesina (2015) in their investigation of groundwater potential and aquifer vulnerability within Akure Southwestern Nigeria. It was inferred from their findings that the study area is characterized mainly by low protective capacity making the location very prone to infiltration. Eyankware et al. (2020) also stated that the lithologic units with a high value of S offer a reliable protective capacity, while geologic formations with a low value of S often have weak or poor protective capacity. Figure 2 presents a spatial distribution map of S of the study area. Longitudinal conductance values that were calculated from

first-order geoelectric indices have values that vary from 0.05 mhos at VES 12 to 1.03 mhos at VES 10 with an average of 0.64. The highest value of S was realized in the north-western area of the map with the value of $1.03 \Omega^{-1}$ at VES 10 (Fig. 2a). Meanwhile, a low value of S could be found in the area around VES 12 and VES 5, which indicates an incompetent or weak zone of aquifer protective capacity that could lead to the infiltration of the aquiferous units (Olusegun et al. 2016). This implies that the protective capacity is high in a zone where the longitudinal conductance is high or vice versa. Eyankware et al. (2022) observed a similar result during their research work on the delineation of aquifer vulnerability in the southeast part of Nigeria.

Transverse unit resistance (Tr)

It is used to delineate the most prolific area of groundwater potential for hydrogeological investigation (Nafez et al. 2010; Eyankware et al. 2022). Longitudinal conductance determines the properties of the conducting layers, while transverse resistance determines the properties of the resistive layers (Yungul 1996). Tr is strongly related to transmissivity. According to Eyankware and Aleke (2021), larger Tr values usually represent higher aquifer transmissivity values. From Fig. 3, Tr ranges from 659.9 to $12.416.65 \Omega m^2$ at VES 8 and VES 10, respectively, with an average of $3888.06 \Omega/m^2$. The region around VES 10

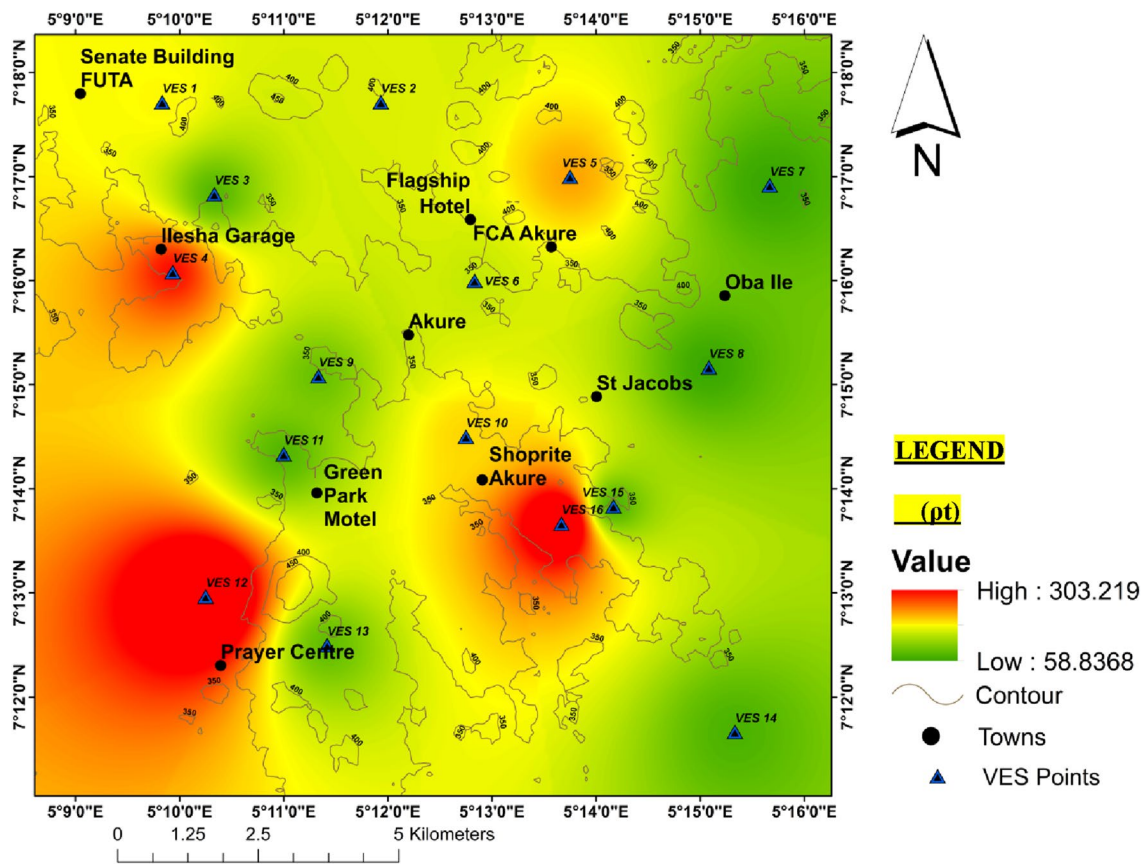


Fig. 5 Spatial distribution map of average transverse resistance

and VES 16, which are the middle northwestern and down southeastern flanks, respectively, of the study area are characterized by relatively high transverse unit resistance, while VES 8, VES 7, VES 15, VES 3, VES 11, and VES 14 have very low Tr. It was observed that Tr is high in the middle NW zone of the study area, which connotes that groundwater potential in the area is expected to be hydrogeologically promising with thick aquifer thickness. However, areas around VES 8, 14, 11, 15, and 16 show low Tr. Such areas are not expected to have high groundwater potential.

Average longitudinal resistance (ρ_L)

The value of longitudinal resistance ranges from 28.21 to 279.51.4 Ω-m with an average value of 85.21 Ω-m as shown in Table 2. A spatial variation map of ρ_L was generated using the values of longitudinal resistivity of the 16 sounding points obtained from the study area as seen in Fig. 4. According to George (2021), the longitudinal resistance helps to assess the rate at which aquiferous units could be prone to infiltration. He stated further that ρ_L can help to determine the direction of conductivity with depth due to its sensitivity to geologic units. In addition, it was observed

that an increase in thickness with depth results in a decrease in longitudinal resistivity with depth, and ρ_L reveals the rate of uniformity with the layer around it. Figure 4 shows that high ρ_L was observed in the southwest and northwest axis of the study area, which implies that the aforementioned tends to high conductivity with depth. This can be attributed to geological units within the area. Furthermore, Eyankware and Aleke (2021) and Gupta et al. (2015) believed that the ρ_L contour can be used to demarcate the saline, brackish, and freshwater aquifers into three different regions based on their varying resistivity regimes.

Transverse resistivity (ρ_t)

Figure 5 reveals that selected parts of southwest, northwest, and southeast have high ρ_t when compared to other parts of the study area. This can be attributed to the resistivity of subsurface rocks such as granite within the aforementioned area which tends to control the resistivity of rock within the area. Table 2 shows that VES 7 has a ρ_t value of 58.82, and VES 12 has a ρ_t value of 303.26, with an average of 136.0683. This means that genuine resistivity normal to the stratification plane, such as shale, is greater than true

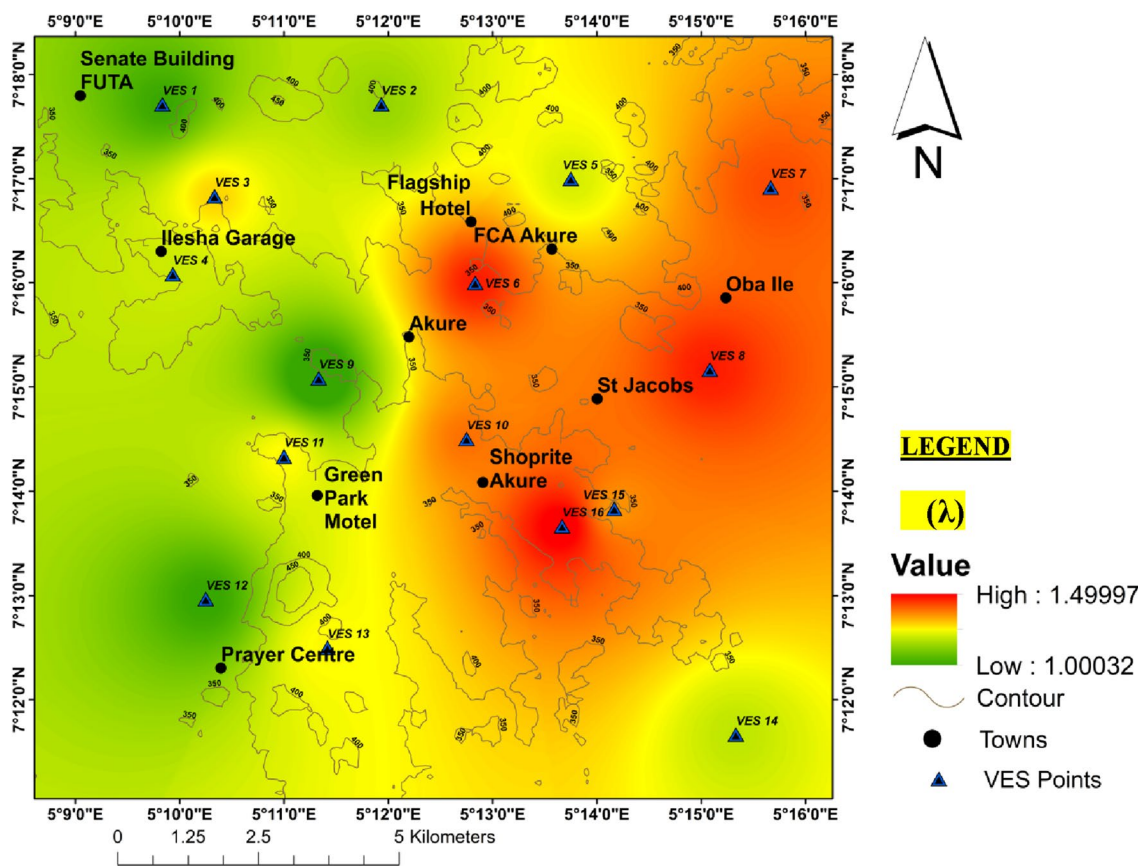


Fig. 6 Spatial variation of the coefficient of anisotropy

resistivity parallel to the stratification plane (Dewashish et al. 2014).

Coefficient of anisotropy (λ)

According to these computations, the coefficient of anisotropy ranges from 1.0 at VES 9 to 1.50 at VES 16, illustrating the genuine variance of the anisotropic character of rock formations (Eyankware and Aleke 2021).

According to Olayinka and Oyedele (2019), Keller and Frischnecht (1966), high anisotropy values are an indication of low porosity and permeability, which implies that such areas are of low hydrogeological viability. However, areas of low anisotropy values connote high porosity and permeability with some degree of fractures at a certain depth. From Fig. 6, it could be observed that VES 8, VES 7, and VES 10, which are located in the northwestern parts of the study area, and VES 6 at the northeastern flanks of the study showed high anisotropy values. Hence, they are not hydrogeologically promising. However, VES 9, VES 1, and VES 12 have low anisotropy values, which imply that they have high porosity and permeability. Therefore, they are

hydrogeologically viable. This is in contrast to the observation of Eyankware 2019 in the sedimentary terrain; those areas with high values of anisotropy show that the fracture system must have extended in all directions with varying degrees of fracturing, resulting in higher porosity from all directions of the fractures within the rock.

Reflection coefficient (R_c)

According to Umayah and Eyankware (2022), the reflection coefficient (R_c) is a measurement of the difference in density between layers of a formation in a given area. It may also reflect the degree of the aquifer fracture. The fracture or freshness of the bedrock is determined by the reflection coefficient. Olayinka (1996) proposed a formula for calculating the reflection coefficient for each VES station, which was adapted from seismic theory. He claimed that the freshness of the basement grows when the reflection coefficient value at any VES point approaches the maximum value of 1. Basement resistivity alone may not be sufficient to identify a promising aquiferous zone inside the basement terrain; consequently, the reflection coefficient must be taken into account to achieve a better outcome in terms of fracture or

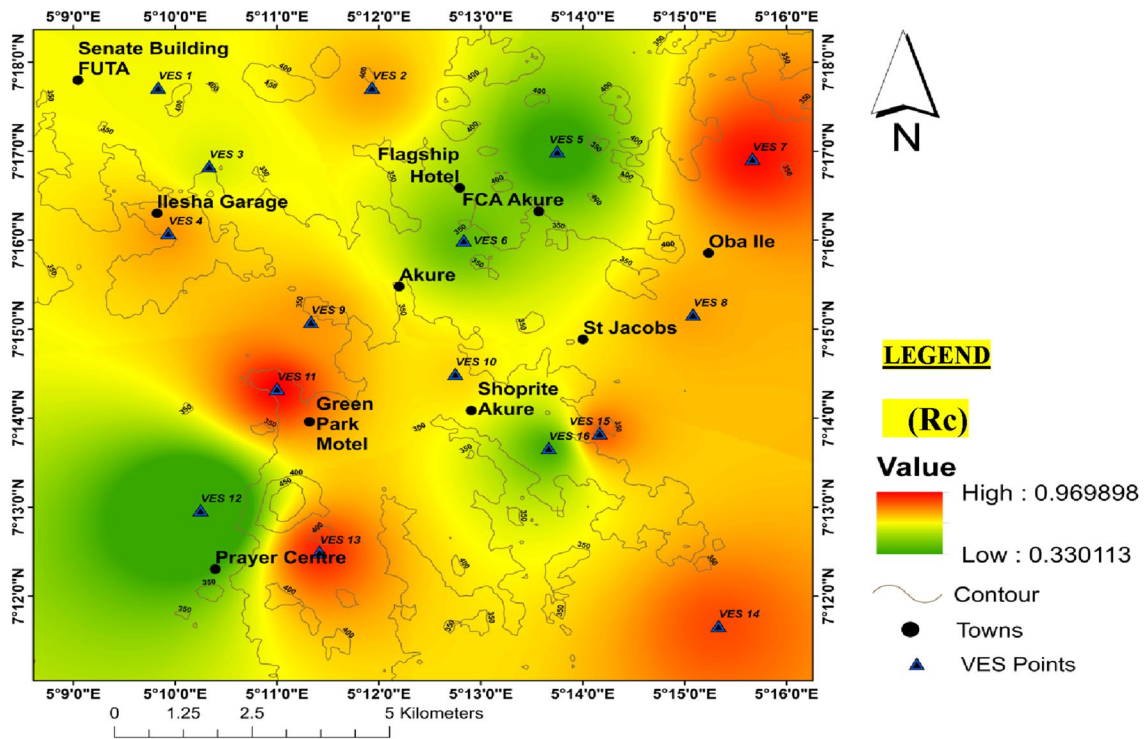


Fig. 7 Spatial distribution map of reflection coefficient

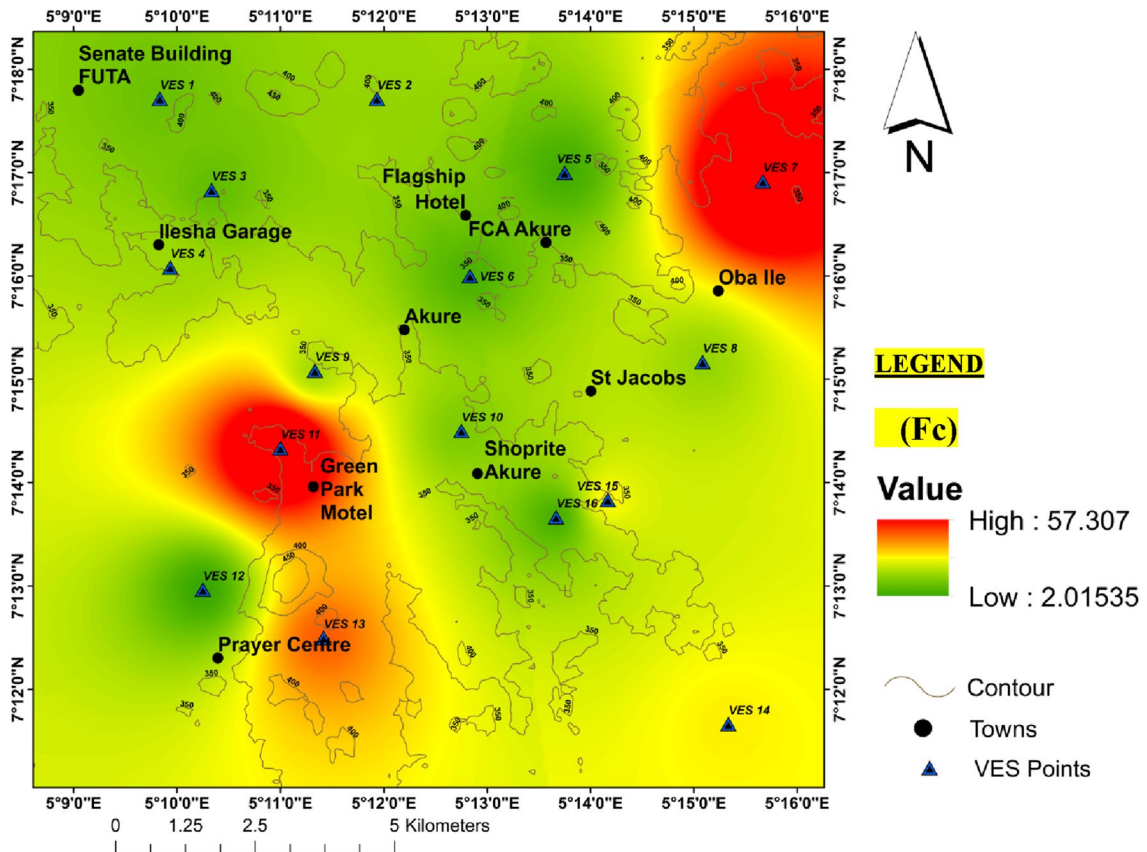


Fig. 8 Spatial variation of resistivity contrast

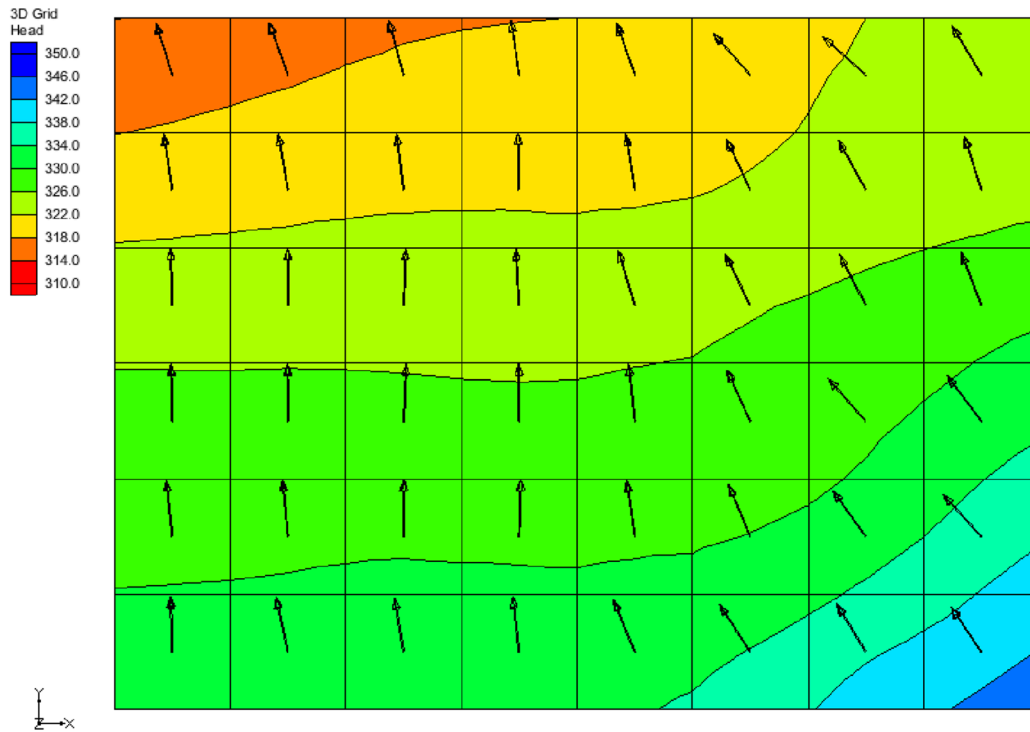


Fig. 9 Groundwater flow model of layer 2 of the study area

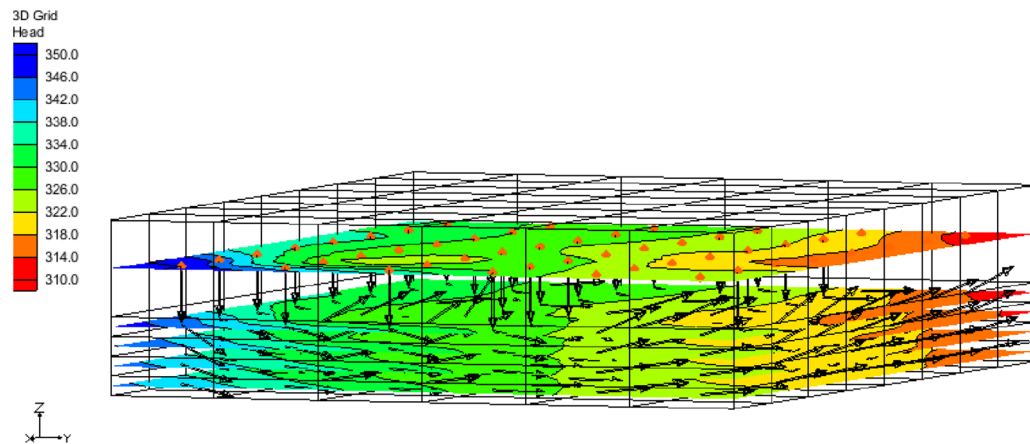


Fig. 10 3D groundwater flow model of the generated five layers in the study area

bedrock freshness. Such a place can be deemed a suitable aquiferous zone if the reflection coefficient is low, less than 0.75, and the overburden thickness is comparatively thick, greater than 25 m. The reflection coefficient map (Fig. 7) shows that the northern section of the study area has a high reflection coefficient, which corresponds to the part of the study area that is underlain by granite rock and also the part of the southwestern part that is underlain by granite gneiss.

Resistivity contrast (F_c)

Resistivity contrast (F_c) provides information on the area of water-bearing potential, while low resistivity contrast values indicate high groundwater potential (Adeniji et al. 2013). For this study, the estimated value of F_c ranges from 2.01 to 57.33. Adeniji et al. (2013) believed that an area with a low value of F_c might indicate an aquiferous unit. From Fig. 8,

it was observed that about 80% of the study area has low resistivity contrast between 2.1 and 20.7, which are VES 1, VES 2, VES 3, VES 4, VES 5, VES 6, VES 8, VES 9, VES 10, VES 12, VES 14, VES 15 and VES 16, while the remaining 20% VES points have relatively high resistivity contrast. This implies that the study area is a hydrogeological viable.

Variation of curve type within the study area

VES findings revealed geoelectric layers ranging from three to six layers with various intra-facies and inter-facies alterations. The curve types depicted by the interpreted curve matching results are HKH, H, A, and QH, where the H curve implies $\rho_1 > \rho_2 < \rho_3$, the K curve connotes $\rho_1 < \rho_2 > \rho_3$, and the Q curve depicts $\rho_1 > \rho_2 > \rho_3$, while the A curve implies $\rho_1 < \rho_2 < \rho_3$. The difference in curve types demonstrated that the study area is heterogeneous in character, and layer qualities and non-uniformity have resulted in subsurface anomalies such as fracturing, weathering, partial weathering, and erosion (Akakuru et al. 2023). The main curve type in the study area is H which is composed of about 69%, while others are HKH (19%), A (6%), and QH (6%). From the interpreted data of all the sounding points in the study area, it was discovered that the subsurface geologic formations comprise three, four, and five layers. It was deduced from the result of the findings that layer model H is the most prominent in the study area, occurring 11 times, which is followed by layer model HKH occurring 3 times, while layer model A and QH occurred only once; see Table 1.

Groundwater modeling

Figure 9 represents one of the layers of the groundwater flow model in the study area generated using the GMS software. It could be deduced that the groundwater flows from the south/southeastern flank to the north/northwestern part of the study area. This implies that the groundwater potential will be higher toward the north/northwestern direction of the study area compared to the other parts. This corroborates with the low anisotropic values Fig. 6 as seen in the north/northwestern flank, which is an indication of high porosity and permeability, resulting in high hydrogeological viability. The transverse unit resistance map revealed that the northwestern part of the area is of high hydrogeological potential, with is in line with the result of the GMS obtained in the study area, while the average longitudinal resistance (ρ_L) reveals that the south/southeastern part of the study area is highly conductive, which is also in agreement with the result obtained from the GMS. Figure 10 shows the groundwater flow direction of the generated five layers and it reveals that the groundwater in the study area tends to all flow in the same direction (i.e., from south/southeast to north/northwest part).

Conclusion

Sixteen (16) VES were performed to identify the subsurface layer parameters (resistivity, depths, and thicknesses) that were used in determining Akure groundwater potential and aquifer vulnerability. Schlumberger electrode configuration was used for the survey, with a maximum half potential electrode separation of 10 m and a maximum half current electrode spacing of 100 m. Four curve types were identified in this study: HKH, H, A, and QH. The interpreted geoelectric data revealed variations in the aquifer and Dar Zarrouk characteristics. According to the study, 39% of the studied area has low water-carrying potential, while 36 and 25% have extremely low and moderate water-bearing potential, respectively. The area's groundwater potential is generally modest, while the northern and western parts of the study area tend to have higher groundwater potential when compared to other parts in the study area as revealed by most of the maps generated. To enhance the existing groundwater resources in the study area, artificial recharging strategies, such as trenches, check dams, and percolation, are recommended.

Declarations

Conflict of interest Every corresponding author certifies that there are no conflicts of interest on behalf of all authors. There are no actual or potential conflicts involving the work.

Data availability My manuscript has associated data in a data repository.

References

- Abiola O, Enikanselu PA, Oladapo MI (2009) Groundwater potential and aquifer protective capacity of overburden units in Ado-Ekiti, Southwestern Nigeria. *Int J Phys Sci* 4:120–132
- Aboh HO, Osazuwa IB (2000) Lithological deductions from regional geoelectric investigation in Kaduna, Kaduna State Nigeria. *Niger J Phys* 12:1–7
- Adedipe OA, Muraina M, Taiwo OA, Adenike AO (2014) Geoelectric investigation of Araromi Area of Akure, Southwestern Nigeria. *J Environ Earth Sci* 4(21):170–181
- Adeniji AE, Obiora DN, Omonona OV, Ayuba R (2013) Geoelectrical evaluation of groundwater potentials of Bwari basement area, Central Nigeria. *Int J Phys Sci* 8(25):1350–1361
- Akakuru OC, Eyankware MO, Akakuru OU, Nkwoada AU, Agunanne VC (2023) Quantification of contamination, ecological risk index, and health risk assessment of groundwater using artificial neural network and multi-linear regression modeling approaches within Egbema, Nigeria. *Arab J Geosci* 16(9):507. <https://doi.org/10.1007/s12517-023-11600-0>
- Akindeji OF (2020) Groundwater aquifer potential using electrical resistivity method and porosity calculation: a case study. *NRIAG J Astron Geophys* 9(1):168–175. <https://doi.org/10.1080/20909977.2020.1728955>

- Akinrinade OJ, Adesina RB (2015) Hydrogeophysical investigation of groundwater potential and aquifer vulnerability prediction in basement complex terrain—a case study from Akure, Southwestern Nigeria. Professional paper RMZ-M&G, 2016, vol 63, pp 1–0005
- Akinseye (2010) Climate variability and effects of weather elements on cocoa and cashew crops in Nigeria. M.Tech Thesis, Unpublished
- Akinseye FM, Ogunjobi KO, Okogbue EC (2012) Climate variability and food crop production in Nigeria. *Int J Acad Res Part A* 4(5):107–111. <https://doi.org/10.7813/2075-4124.2012/4-5/A.13>
- Akintorinwa OJ (2015) Groundwater potential assessment of Iwaro-Oka, SW Nigeria using geoelectric parameters. *Br J Appl Sci Technol* 6(4):364–377
- Akpan AE, Ugbaja AN, George NJ (2013) Integrated geophysical, geochemical and hydrogeological investigation of shallow groundwater resources in parts of the Ikom-Mamfe Embayment and the adjoining areas in Cross River State, Nigeria. *J Environ Earth Sci* 70:1435–1456
- Akpan AE, Ebong DE, Ekwok SE, Joseph S (2014) Geophysical and geological studies of the spread and industrial quality of Okurike Barite deposit. *Am J Environ Sci* 10(6):566–574
- Al-Garni MA, Hassanein HI, Gobashy M (2005) Ground-magnetic survey and Schlumberger sounding for identifying the subsurface factors controlling the groundwater flow along Wadi Lusab, Makkah Al-Mukarramah, Saudi Arabia. *Egypt J Appl Geophys* 4:59–74
- Asfahani J (2013) Groundwater potential estimation using vertical electrical sounding measurements in the semi-arid Khanasser Valley region, Syria. *Hydrol Sci J* 58:468–482
- Ayolabi EA, Adedeji JK, Oladapo MI (2003) A geoelectric mapping of Ijapo, Akure southwest Nigeria and its hydrogeological implications. *Glob J Pure Appl Sci* 10(3):441–446
- Carrarad N, Willets J, Tim F (2019) Groundwater as a source of drinking water in Southeast Asia and the Pacific: a multi-country review of current reliance and resource concerns. <https://doi.org/10.3390/w11081605>
- Dan-Hassan MA, Olorunfemi MO (1999) Hydrogeological investigation of a basement terrain in the North-Central part of Kaduna State. *Niger J Min Geol* 35(2):189–206
- Dewashishe K, Rai SN, Thiagarajan S, Kumari YR (2014) Evaluation of heterogeneous aquifers in hard rocks from resistivity sounding data in parts of Kalmeshwar Taluk of Nagpur District, India. *CurrSci* 107:1137–1145
- Durotoye AA, Osisanya OW, Saleh AS, Maruff AB (2022) Identification of potential and aquifer vulnerability in basement terrain of southern Nigeria, using geophysical approach. *World Sci News WSN* 173(2022):128–148
- Ebong ED, Akpan AE, Onwuegbuche AA (2014) Estimation of geohydraulic parameters from fractured shales and sandstone aquifers of Abi (Nigeria) using electrical resistivity and hydrogeologic measurements. *J Afr Earth Sci* 96:99–109
- Ebong DE, Akpan AE, Emeka CN, Urang JG (2016) Groundwater quality assessment using geo-electrical and geochemical approaches: case study of Abi area, south-eastern Nigeria. *Appl Water Sci*. <https://doi.org/10.1007/s13201-016-0439-7>
- Eebo FO, Yusuf GA (2021) Geophysical investigation of groundwater potential of a site in Obale area of Akure, Nigeria. *Int J Eng Appl Sci Technol* 6(1):88–93
- Eyankware MO (2019) Integrated Landsat imagery and resistivity methods in evaluation of groundwater potential of fractured shale at Ejekwe area, Southeastern Nigeria. Unpublished PhD Thesis
- Eyankware MO, Akakuru CO (2022) Appraisal of groundwater to risk contamination near an abandoned limestone quarry pit in Nkalagu, Nigeria, using enrichment factor and statistical approaches. *J Energy Water Resour*. <https://doi.org/10.1007/s42108-022-00186-0>
- Eyankware MO, Aleke G (2021) Geoelectric investigation to determine fracture zones and aquifer vulnerability in southern Benue Trough southeastern Nigeria. *Arab J Geosci*. <https://doi.org/10.1007/s12517-021-08542-w>
- Eyankware MO, Umayah SO (2022) 1D modeling of aquifer vulnerability and soil corrosivity within the sedimentary terrain in Southern Nigeria, using resistivity method. *World News Nat Sci* 41:33–50
- Eyankware MO, Aleke CG, Selema AOI, Nnabo PN (2020) Hydrogeochemical studies and suitability assessment of groundwater quality for irrigation at Warri and environs, Niger delta basin, Nigeria. *Groundw Sustain Dev* 10:100293
- Eyankware MO, Akakuru CO, Eyankware EO (2022) Hydrogeophysical delineation of aquifer vulnerability in parts of Nkalagu areas of Abakaliki, SE, Nigeria. *Sustain Water Resour Manag*. <https://doi.org/10.1007/s40899-022-00603-6>
- George NJ (2021) Modelling the trends of resistivity gradient in hydrogeological units: a case study of alluvial environment. *Model Earth Syst Environ*. <https://doi.org/10.1007/s40808-020-01021-3>
- Gupta G, Patil SN, Padmane ST, Erram VC, Mahajan SH (2015) Geoelectric investigation to delineate groundwater potential and recharge zones in Suki River basin, north Maharashtra. *J Earth Syst Sci* 124(7):1487–1501
- Henriet JP (1976) Direct application of Dar Zarrouk parameters in ground water survey. *Geophys Prospect* 24:344–353
- Joel ES, Olasehinde PI, De DK, Omeje M, Adewoyin OO (2016) Estimation of aquifer transmissivity from geo-physical data. A case study of covenant University and environs, Southwestern Nigeria. *Sci Int (lahore)* 28(4):3379–3385
- Kazeem AS (2007) Lithostratigraphy of Nigeria: an overview. In: Workshop on geothermal reservation engineering, Stanford University, Stanford, California, USA, vol 32, pp 1–4
- Kearey P, Brooks M, Hill I (2002) An introduction to geophysical exploration, 3rd edn. Blackwell Science Ltd Editorial Offices, Oxford
- Keller GV, Frischnecht FC (1966) Electrical methods in geophysical prospecting. Pergamon Press, Oxford, p 523
- Loke MH (1999) A practical guide to 2D and 3D surveys. In: Electrical imaging surveys for environmental and engineering studies. Course note, vol 1, pp 8–10
- Maillet R (1947) The fundamental equations of electrical prospecting. *Geophysics* 12(4):529–556. <https://doi.org/10.1190/1.1437342>
- Nafez H, Kaita H, Samer F (2010) Calculation of transverse resistance to correct aquifers resistivity of groundwater saturated zones: Implication for estimated its hydrogeological properties. *Leban Sci J* 11(1):105–115
- Nwachukwu SR, Bello R, Ayomide O, Balogun AO (2019) Evaluation of groundwater potentials of Orogun, South-South part of Nigeria using electrical resistivity method. *Appl Water Sci* 9:184. <https://doi.org/10.1007/s13201-019-1072-z>
- Nwanko C, Nwasu L, Emujakporue G (2011) Determination of Dar Zarouk parameters for assessment of groundwater potential: case study of Imo State, southeastern Nigeria. *J Econ Sustain Dev* 2:57–71
- Obasi PN, Ekinya EA, Eyankware MO (2022) Reliability of geophysical techniques in the evaluation of aquifer at Igbo-Imabana, Cross River State, Nigeria using electrical resistivity method. *Water Resour J* 32(1):105–121
- Odusanya BO, Amadi UNP (1990) An empirical resistivity model for predicting shallow groundwater in the Basement Complex Water Resources. *J Nig Ass Hydrogeol* 2:77–87
- Oladapo MI, Akintorinwa OJ (2007) Hydrogeophysical study of Ogbese, southwestern. *Niger Glob J Pure Appl Sci* 13(1):55–56

- Oladapo MI, Mohammed MZ, Adeoye OO, Adetola BA (2004) Geoelectrical investigation of the Ondo State Housing Corporation Estate, Ijapo Akure, Southwestern Nigeria. *J Min Geol* 40:41–48. <https://doi.org/10.4314/jmg.v40i1.18807>
- Oladunjoye MA, Jekayinfa S (2015) Efficacy of Hummel (modified Schlumberger) arrays of vertical electrical sounding in groundwater exploration: case study of parts of Ibadan Metropolis, southwestern Nigeria. *Int J Geophys*. <https://doi.org/10.1155/2015/612303>
- Olayinka AI (1996) Non-uniqueness in the interpretation of bedrock resistivity from sounding curves and its hydrogeological implications. *Water Resour J Niger Assoc Hydrogeol* 7(1 & 2):49–55
- Olayinka AI, Oyedele EAA (2019) On the application of coefficient of anisotropy as an index of groundwater potential in a typical basement complex of Ado Ekiti, Southwest, Nigeria. *Phys Sci Int J* 22(1):1–10
- Oli IC, Ahairakwem CA, Opara AI (2021) Hydrogeophysical assessment and protective capacity of groundwater resources in parts of Ezza and Ikwo areas, southeastern Nigeria. *Int J Energy Water Res* 5:57–72. <https://doi.org/10.1007/s42108-020-00084-3>
- Olorunfemi MO, Fasuyi SA (1993) Aquifer types and the geoelectric/hydrogeologic characteristics of part of central basement terrain of Nigeria (Niger State). *J Afr Earth Sc* 16:309–317. [https://doi.org/10.1016/0899-5362\(93\)90051-Q](https://doi.org/10.1016/0899-5362(93)90051-Q)
- Olorunfemi MO, Okhue EJ (1992) Hydrogeologic and geologic significance of a geoelectric survey at Ile-Ife, Nigeria. *J Min Geol* 28:242–350
- Olorunfemi MO, Ojo JS, Akintunde MO (1999) Hydrogeophysical evaluation of the groundwater potentials of the Akure metropolis. *J Min Geol* 35:207–228
- Olusegun OA, Adeolu OO, Dolapo FA (2016) Geophysical investigation for groundwater potential and aquifer protective capacity around Osun State University (UNIOSUN) College of Health Sciences. *Am J Water Resour* 4(6):137–214
- Oni TE, Omosuyi GO, Akinlalu AA (2017) Groundwater vulnerability assessment using hydrogeologic and geoelectric layer susceptibility indexing at Igbara Oke, Southwestern Nigeria. *NRIAG J Astron Geophys* 6(2017):452–458
- Patrick L, Benoît D, Robert W (2021) Review: Hydrogeology of weathered crystalline/hard-rock aquifers—guidelines for the operational survey and management of their groundwater resource. *Hydrogeol J*. <https://doi.org/10.1007/s10040-021-02339-7>
- Rahaman MA (1988) Recent advances in the study of the basement complex of Nigeria. Precambrian geology of Nigeria. Geological Survey of Nigeria, Kaduna South, pp 11–43
- Suneetha N, Gupta G (2018) Evaluation of groundwater potential and saline water intrusion using secondary geophysical parameters: A case study from western Maharashtra India. *E3S Web Conf* 54:00033. <https://doi.org/10.1051/e3sconf/20185400033>
- Umayah OS, Eyankware MO (2022) Aquifer evaluation in southern parts of Nigeria from geo-electrical derived parameters. *World News Nat Sci* 42:28–43
- United Nations World Water Development Report (UNESCO) (2022) Groundwater: making the invisible visible
- Yungul SH (1996) Electrical methods in geophysical exploration of sedimentary basins. Chapman & Hill, London
- Zohdy AA, Eaton CP, Mabey DR (1974) Application of surface geophysical to ground water investigation technology. *Water Resources Investigation*, Washington, US Geological survey

Publisher's Note Springer Nature remains neutral with regard to jurisdictional claims in published maps and institutional affiliations.

Springer Nature or its licensor (e.g. a society or other partner) holds exclusive rights to this article under a publishing agreement with the author(s) or other rightsholder(s); author self-archiving of the accepted manuscript version of this article is solely governed by the terms of such publishing agreement and applicable law.